

EPA-650/2-74-046-b

July 1974

Environmental Protection Technology Series

**DEVELOPMENT OF A GAS LASER SYSTEM
TO MEASURE TRACE GASES
BY LONG PATH
ABSORPTION TECHNIQUES:
VOLUME II - FIELD EVALUATION OF GAS LASER
SYSTEM FOR OZONE MONITORING
FINAL REPORT**



Office of Research and Development
U.S. Environmental Protection Agency
Washington, DC 20460

**DEVELOPMENT OF A GAS LASER SYSTEM
TO MEASURE TRACE GASES
BY LONG PATH
ABSORPTION TECHNIQUES:
VOLUME II - FIELD EVALUATION OF GAS LASER
SYSTEM FOR OZONE MONITORING
FINAL REPORT**

by

W. A. McClenny, F. W. Baity, Jr.,
R. E. Baumgardner, Jr., and R. A. Gray

Chemistry and Physics Laboratory
National Environmental Research Center
Research Triangle Park, North Carolina 27711

and

R. J. Gillmeister and L. R. Snowman

General Electric Company
Electronic System Division
100 Plastics Avenue
Pittsfield, Massachusetts 01201

Contract No. 68-02-0757
ROAP No. 26ACX
Program Element No. 1AA010

EPA Project Officer: W. A. McClenny

Prepared for

OFFICE OF RESEARCH AND DEVELOPMENT
U.S. ENVIRONMENTAL PROTECTION AGENCY
WASHINGTON, D.C. 20460

July 1974

This report has been reviewed by the Environmental Protection Agency and approved for publication. Approval does not signify that the contents necessarily reflect the views and policies of the Agency, nor does mention of trade names or commercial products constitute endorsement or recommendation for use.

TABLE OF CONTENTS

	<u>Page No.</u>
A. INTRODUCTION	1
B. DESCRIPTION OF THE SYSTEM	3
C. SYSTEM CALIBRATION	10
D. PATH-POINT MONITOR COMPARISON METHODOLOGY	14
E. FIELD MEASUREMENT RESULTS	31
F. CONCLUSIONS	43
G. REFERENCES	46

LIST OF ILLUSTRATIONS

	<u>Page No.</u>
Figure 1 - ILAMS Block Diagram	4
Figure 2 - "V" Laser Optical Layout	6
Figure 3 - Data Collection and Reduction System	9
Figure 4 - Response to Ozone in Calibration Cell	12
Figure 5 - Space-Time Plane for Measurement Path	17
Figure 6 - Time-Delayed Correlation Between Ozone Point Monitors	21
Figure 7 - Ambient Ozone Variations About Mean Ozone Concentrations	23
Figure 8 - Open-Path Measurement Site	24
Figure 9 - Super-Imposed Recorder-Traces	27
Figure 10 - Super-Imposed Recorder-Traces (Space)	29
Figure 11 - Super-Imposed Recorder-Traces (Time)	30
Figure 12 - ILAMS and Auxiliary Equipment in Trailer	32
Figure 13 - A View of the Optical Path Over Which Ozone was Measured	33
Figure 14 - Comparison by Use of Procedure 3	36
Figure 15 - System Performance Effect from Beam Movement on the Retroreflector	38
Figure 16 - Comparative Path/Moving Point Monitor Ozone Data	41
Figure 17 - Point and Path Monitor Comparison	44

LIST OF TABLES

Table I Syracuse N. Y. Ozone Concentrations	2
Table II Characterization of Ozone Variability Along Measurement Path	26
Table III Point Monitor-Path Monitor Comparison Data by Procedure 1	34
Table IV Shift of Beam Position on Retroreflector with Time of Day as Indicated by Focusing Lens Adjustment	42

A. INTRODUCTION

The Final Report of EPA Contract 68-02-0757, Development of a Gas Laser System to measure Trace Gases by Long Path Absorption Techniques, consists of two (2) volumes:

- I. Gas Laser System Modifications for Ozone Monitoring
- II. Field Evaluation of Gas Laser System for Ozone Monitoring

The work reported here stems from development activity begun in 1966 at General Electric's Electronics Laboratory. Under this contract, a breadboard laser long path monitor called ILAMS (Infrared Laser Atmospheric Monitoring System) was modified to improve its sensitivity as indicated by previous field experience. System parameters were selected to optimize system performance for ozone monitoring. A field evaluation of the modified system was conducted.

Following completion of the system design investigations and hardware modifications described in Volume I of the Final Report, the laser path monitor called ILAMS was set up and operated over a range (one way distance) of .67 kilometer. Field tests were performed in cooperation with EPA personnel. The object was to evaluate the monitoring capability of the breadboard ILAMS by comparing its ambient air measurement of ozone concentrations with data from chemiluminescence point monitors operated near the system's optical path. Table I shows representative chemiluminescence ozone monitor data from Syracuse, New York, where the measurements were made.

This portion (Volume II) of the Final Report, is a joint EPA-General Electric Company effort. In the sections which follow, the system is described. Calibration of the system with a multipass cell and point/path monitor comparison methodology are discussed, field test results are presented and conclusions are given.

Month + Year		Monitoring Station			
		No. 1		Downtown	
		Average of Daily Averages	Range of Maximum Hourly Averages	Average of Daily Averages	Range of Maximum Hourly Averages
Jan	1973	10	5 - 35	8	5 - 29
Feb	1973	15	0 - 40	11	5 - 57
Mar	1973	14	1 - 48	14	6 - 96
Apr	1973	20	14 - 59	19	12 - 108
May	1973	21	17 - 75	18	10 - 76
June	1973	27	16 - 87	*	24 - 124
July	1973	35	20 - 125	39	30 - 132
Aug	1973	32	30 - 100	34	22 - 132
Sept	1973	17	9 - 93	no data	
Oct	1973	11	15 - 57	no data	
Nov	1973	9	9 - 49	no data	
Dec	1973	10	2 - 32	no data	
Jan	1974	9	4 - 32	no data	

Data from New York State Continuous Air Monitoring System

* Number of daily averages (18) insufficient, per New York State data processing criteria, for taking monthly average. Average for 18 days is 36 ppb.

Table I - Syracuse, N. Y. Ozone Concentrations During Recent Months
(in Parts per Billion)

B. DESCRIPTION OF THE SYSTEM

The gas laser system used in this evaluation is a breadboard instrument. It was constructed by General Electric Company under an internally funded program and its performance evaluated in rural and urban atmospheres under EPA Contract EHSD 71-8. Under this contract the system was modified as described in Volume I of this document. The system operates in the middle region of the infrared spectrum and identifies atmospheric constituents by absorption spectroscopy. It measures average pollutant concentrations (total burden) over its optical path. Laser operation is at relatively low, safe power densities of .001 to .01 watts/cm² in the spectral region where the eye does not transmit.

Figure 1 is a block diagram of ILAMS. The output power from the laser is directed to a 50 percent beamsplitter via a 1 mm spatial filter (cleanup aperture). The energy reflected from the beamsplitter is focused down to a 0.1 mm aperture that serves as an attenuator. Behind this aperture is the reference energy detector. The transmitted power through the beamsplitter goes to a germanium lens which focuses the energy near the focal point of an off-axis parabolic mirror, and the expanded, nearly collimated beam is transmitted to the retroreflector. The return energy from the retroreflector retraces the path through the beam-expanding parabolic mirror and the germanium lens to the beamsplitter. The return energy reflected from the beamsplitter is collected by a germanium lens doublet and focused on the signal detector. Preamplifiers are mounted directly behind the signal and reference detectors. The preamp outputs go to the signal processor. The detectors used in the system are thermistor bolometers, operating at ambient temperature (uncooled), having a characteristic flat response across the middle infrared spectral region.

The attenuation of laser energy at many wavelengths produces absorption patterns which are used to separate pollutant absorption from spectral interferences in the signal processor. C¹²O₂¹⁶ laser lines in the P branch of the 00⁰₁ - 02⁰₀

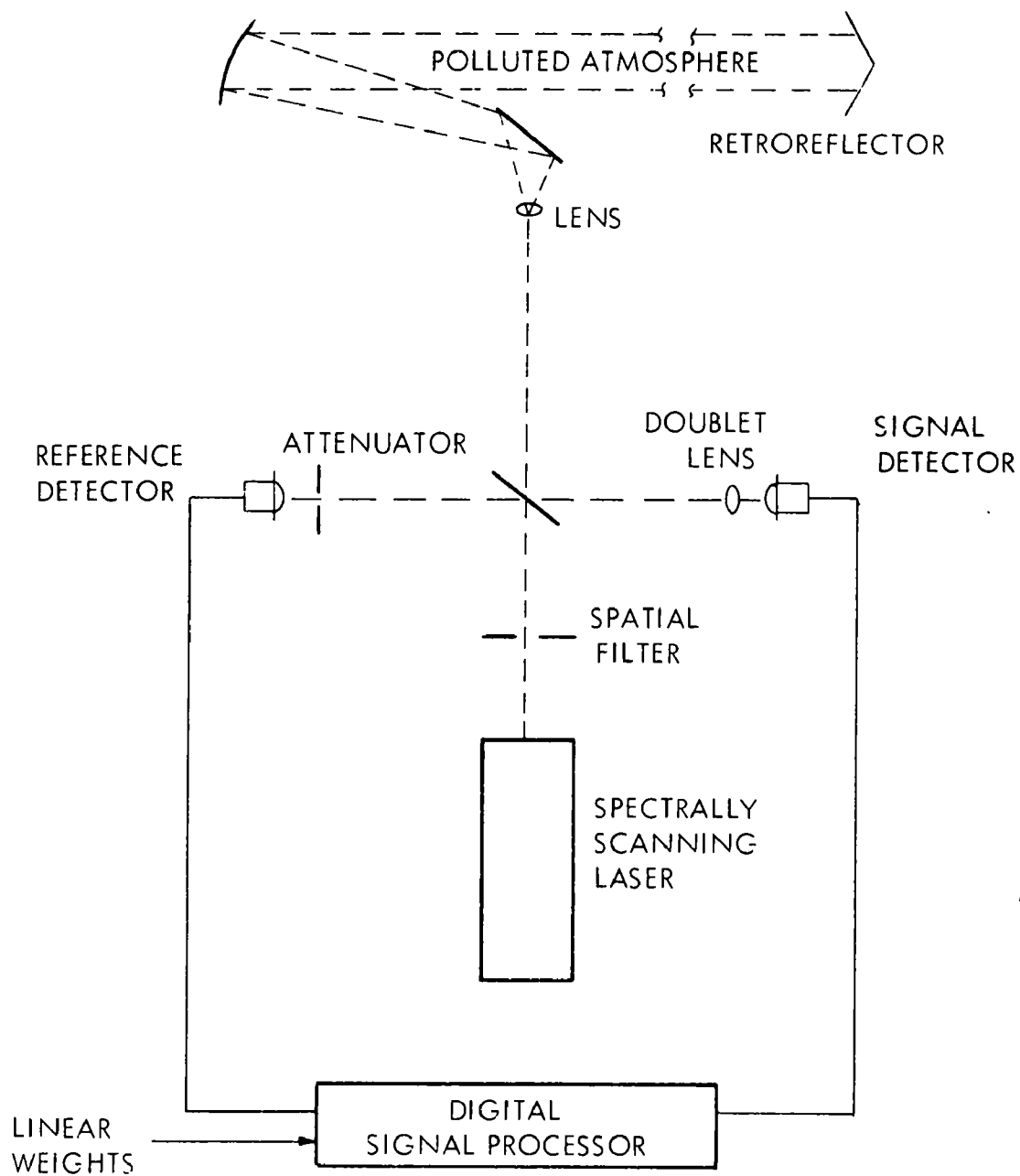


Figure 1. ILAMS BLOCK DIAGRAM

transition lie in the same spectral region as ozone absorption so that coincidences between the two exist. Several of the absorption coefficients recently measured by EPA personnel are listed in Volume I. Prior to the actual monitoring of ambient ozone, a set of four wavelengths, optimized for ozone detection in the presence of other atmospheric attenuators, was chosen by an optimization procedure. This procedure and the calculation of linear weights is described in Volume I. During the course of the evaluation some changes in wavelengths and weights occurred. The final wavelengths were 9.2938, 9.5039, 9.5862 and 10.5321 microns. For these wavelengths the linear weights were respectively -0.4215, 1.0000, -0.5820 and 0.0034.

The spectrally scanning laser itself includes a high gain CO₂ flowing gas laser as the radiation source and a wavelength selection mechanism, which periodically (50 Hz) scans through a series of four laser wavelengths. A typical output scan consists of laser pulses of 2.5 msec. duration separated by time intervals of the same duration during which laser action is interrupted and detector null signals are recorded. The laser optical configuration is shown in Figure 2.

The laser cavity consists of a "V" shaped plasma tube and an external spectral tuner. A relatively long laser cavity is used for sufficient gain to overcome the losses inherent in the spectral tuner and to obtain lasing action on a large number of spectral lines. A beam travels through the plasma tube with aid of a mirror at the point of the "V". Leaving the tube through a germanium Brewster window, the beam is directed by mirrors through an iris (for mode control) and onto a 105 lines/mm diffraction grating, which disperses the beam spectrally and spatially. The four wavelengths of interest are then relayed through holes in the chopper wheel to the four end mirrors of the laser cavity. These holes in the chopper are so located that, as the wheel turns, only one wavelength at a time is permitted to pass through to the end mirrors. The four end or wavelength selection mirrors are adjusted so that the beams are directed back on themselves through the laser cavity. In this way, selected laser wavelengths are transmitted sequentially.

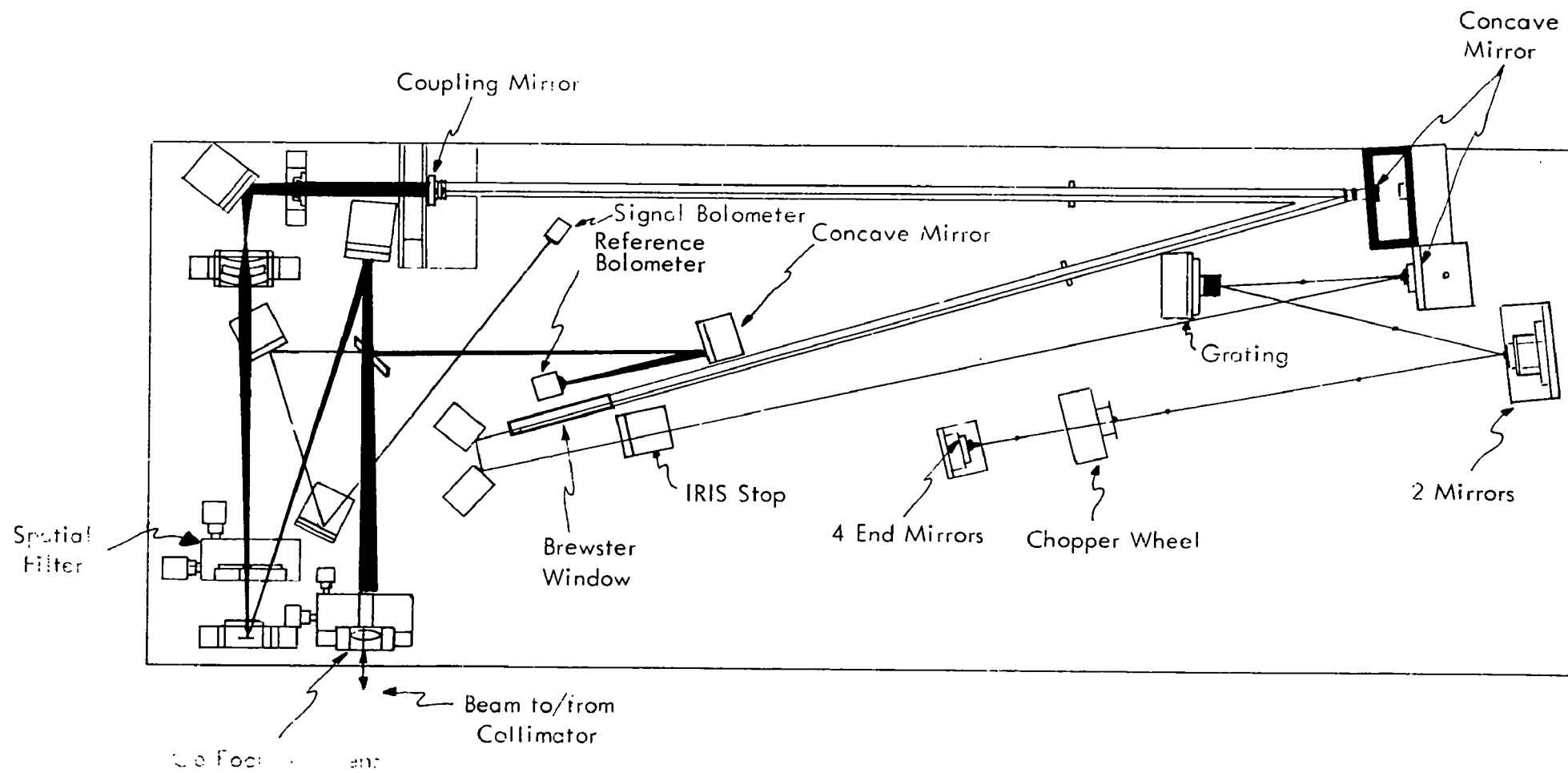


Figure 2. "V" LASER OPTICAL LAYOUT

The mini-computer signal processor includes a general purpose (stored program) mini-computer and appropriate interface electronics. The collection and reduction of data is entirely under computer, i.e., program control; results are displayed on simple displays incorporated in the equipment, and on an optional teletype, which need not be used (or even be connected) during field or test range exercise of the system.

The use of the stored program control and data reduction means:

- changes in system design, or variations in data reduction algorithms, may be accommodated without alteration of the data collection or reduction hardware; only changes in the control program will be required.
- modification of signal processor parameters such as number of wavelengths (up to 8), gate locations, system response time, weighting factors, etc., do not even require software changes, these parameters are expediently entered by the teletype input.
- the precision of data processing may be made as accurate as desired; similarly the impact of imprecise calculations may be assessed by direct simulation for purposes of evaluating future low cost special purpose instruments.
- additional data, e.g., environmental conditions, time, date, signal variability, laser parameters, etc., may be measured and recorded without modification of or addition to the existing system hardware.
- the performance of one or more data processing and display systems can be directly analyzed, e.g., data from several ozone monitors could be crosscorrelated and recorded.

The data collection and reduction system is sketched in Figure 3. A Digital Equipment Corporation PDP 11/05 is used for the central processor. The data collection and reduction equipment in Figure 3 consists of three major subsystems:

Interface Subsystem

This subsystem includes an 8 input analog signal multiplexer, which is followed by a sample-and-hold amplifier and an analog-to-digital converter at 10-bit precision. (The analysis path detector preamplifier output is connected to one multiplexer input, the reference path to a second multiplexer input, the remaining 6 are available for sensing other voltage levels of interest). Additional subsystem elements include an AGC attenuator, a wheel position counter and demultiplexer/storage capability for analog data displays like the meters shown in Figure 3.

Central Processor Subsystem

The central processor and its own control panel form this subsystem. Power supplies for this equipment are contained within the CPU cabinet proper. The central processor control panel ordinarily is disabled during operation.

Program Input and Data Logging Subsystem

A Teletype Corporation ASR-33 teletype with appropriate interface circuits constitutes this subsystem. As indicated, it plays two roles. First, it permits entry (ordinarily via paper tape) of the control program. Second, it permits detailed reporting of directly measured quantities, or derived (computed) quantities.

The central processor is designed so that programs stored in its core memory may be caused to remain intact during periods of no primary power. This option is exercised, so that once a control program has been entered in the CPU, it need not be reentered until there is a need to change it, regardless of whether the CPU remains energized or not. The control program is designed so that it will run properly regardless of whether the teletype is connected or not. Thus the teletype unit is an optional data display device, not an essential component of the system once the control program has been entered.

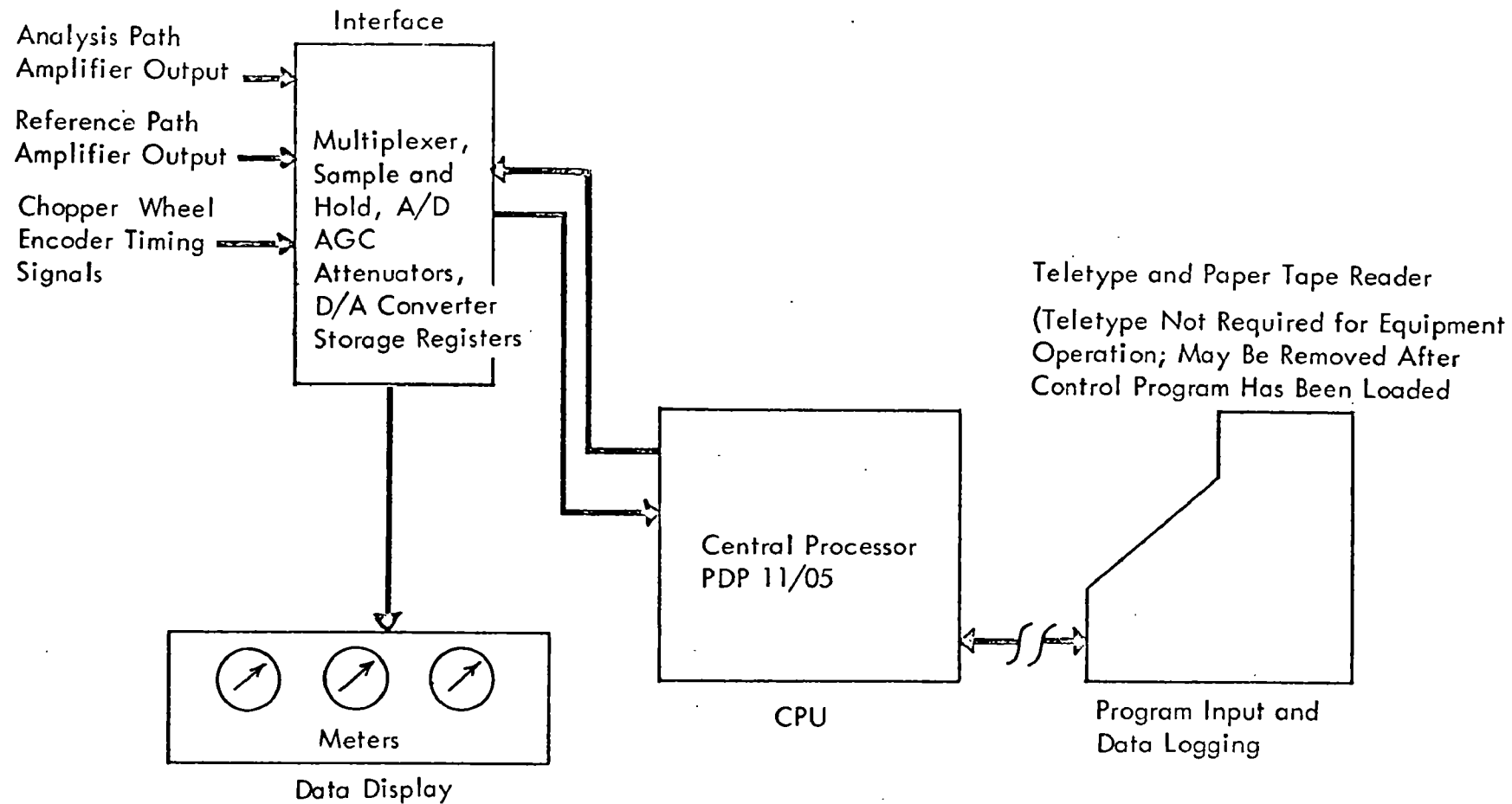


Figure 3. DATA COLLECTION AND REDUCTION SYSTEM

C. SYSTEM CALIBRATION

In day-to-day operation, system zero was set by comparing concentration data on the teletype printout with the readings of a portable chemiluminescent ozone point monitor operated along the system's optical path. An appropriate offset was entered in the signal processor Parameter Table so that the value on the printout corresponded to the average concentration indicated on the point monitor strip chart record.

For ozone, and pollutants with similar diurnal variations, a simple alternative procedure can be followed. Typically, ozone concentrations were zero from sunset until shortly after sunrise. During this period, the system can be zeroed by offsetting to zero the log of transmission at each wavelength. Adding this fixed offset in the signal processor is equivalent to introducing an optical filter that compensates for the fixed absorption pattern introduced by the system optics.

Prior to field operation, the system was calibrated using a multipass (White) cell* into which known ozone concentrations were introduced. In the experimental setup, the uncollimated laser beam was mirror-directed into the entrance port of the multipass cell. Cell mirrors were so aligned that the beam was redirected back on itself, rather than leaving the cell through the exit port. Two small ozone generators employing UV illumination were arranged in series to produce a 1.6 ppm ozone concentration in air flowing into the cell at four liters per minute. This corresponds to 8.0 percent absorption at the strongly absorbing wavelength, $\lambda = 9.505\mu$, and to an equivalent ozone burden along the measurement path of 50 ppb (parts per billion). Ozone concentrations at the entrance and exit of the calibration cell were monitored with a portable chemiluminescence ozone monitor** (Analytical Instrument Development, Inc.) which had been previously calibrated by comparison with an ozone generator, which was in turn calibrated by the neutral buffered potassium iodide technique. No appreciable ozone loss was observed.

*Fabricated by EPA

**EPA contribution to field tests

For another run under the same conditions, the ILAMS was used as the sensor of ozone concentration buildup in the cell. In the system, the teletype printout is the data display device. On the printout each group of digits (five at the time of the experiment but now four) represents the sum of the weighted natural logarithms (ln) of the return signal to reference signal voltage ratios for each of the transmitted wavelengths. This sum is the system response. It is proportional to αCL , the exponent of the Beer's Law equation, where α is the absorption coefficient, C the concentration and L the system's optical path length. Since αCL is dimensionless, the units of α are the reciprocal product of those used for C and L as will be seen below.

For this experiment, the system's four wavelengths (9.305, 9.504, 9.586 and 10.532 microns) were weighted for ozone as the target gas and the sum appeared as the left hand group of digits on the printout. The weights were, respectively, -.4131, 1.0000, -.5869 and zero. As the ozone concentration in the multipass cell increased to an equilibrium value, system response was recorded on the teletype printout. At equilibrium the reading on the teletype printout was 00064, corresponding to an αCL of .128. This compares with an αCL of .119 derived from multipass cell parameters and the point monitor measurement of ozone concentration as shown in the following calculations. Figure 4 shows how ILAMS response and ozone concentration measurements relate, in terms of αCL , as cell ozone concentration increases with time to an equilibrium value. Intermediate points on the plot are determined in the same manner as shown below for equilibrium values.

αCL Calculation from Multipass Cell Parameters

Measured O_3 absorption coefficients, α , at transmitted wavelengths are as follows:

<u>λ</u>	<u>α (atm⁻¹ cm⁻¹)</u>
9.305	0
9.504	12.659
9.586	.69183
10.532	0

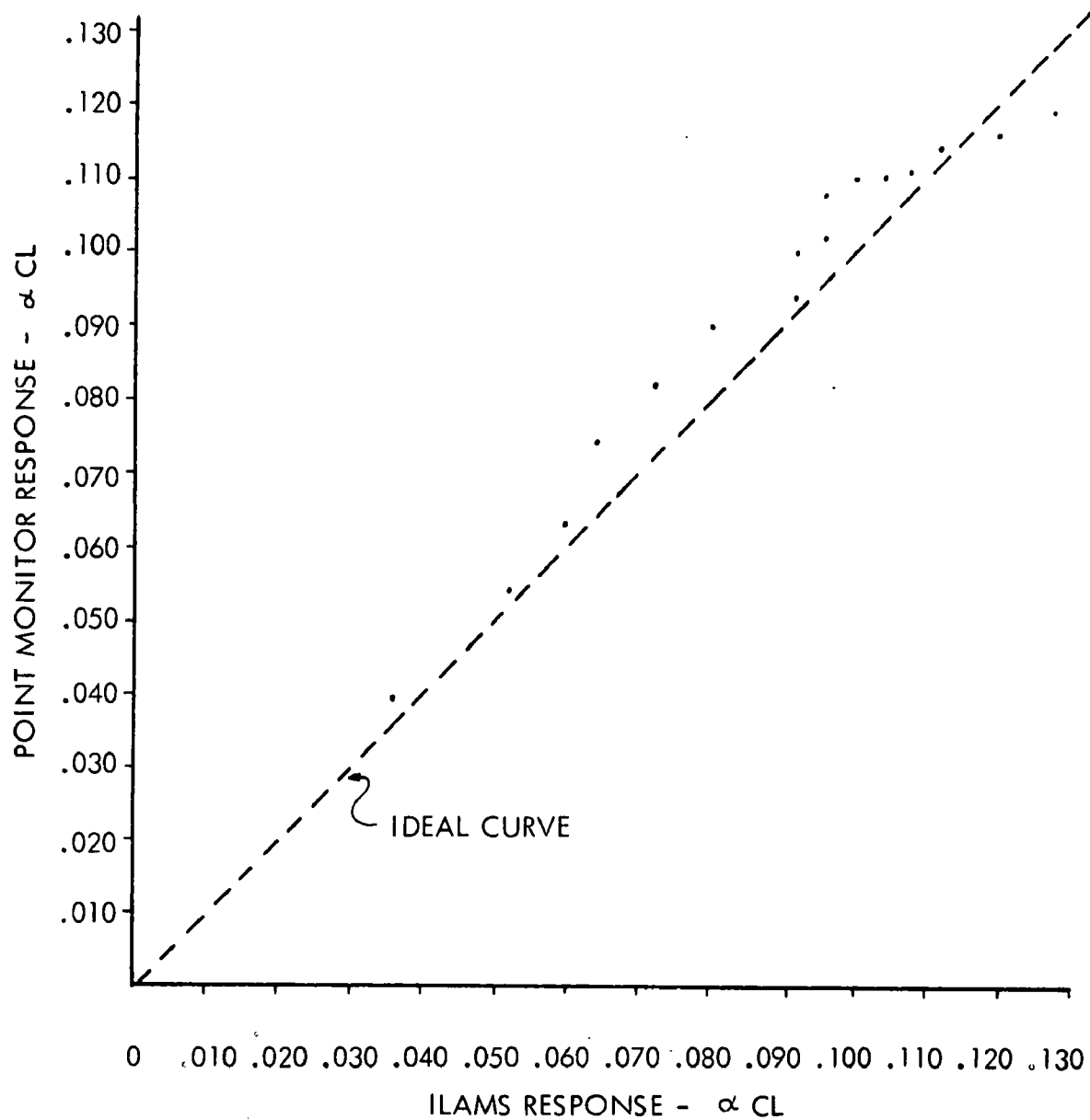


Figure 4. RESPONSE TO OZONE IN CALIBRATION CELL
(ILAMS VS. POINT MONITOR)

The resultant α_r , the sum of weighted absorption coefficients at the four wavelengths is:

$$\begin{aligned}\alpha_r &= 4131 \times 0 + 1.0000 \times 12.659 - .5869 \times .69183 + 0 \times 0 \\ &= 12.253 \text{ atm}^{-1} \text{ cm}^{-1}\end{aligned}$$

The multipass cell was aligned to produce 42 passes through a 5 foot (1.524 meter) cell length. For an assumed 1.52 ppm equilibrium O_3 concentration in the cell (obtained from previous point monitor measurements employing the same procedure) we have:

$$\alpha_r \text{ CL} = 12.253 \times 1.52 \times 10^{-6} \times 42 \times 1.524 \times 100 = .1192$$

D. PATH-POINT MONITOR COMPARISON METHODOLOGY

There are several methods by which comparisons between point monitors and path monitors can be accomplished. For each of these methods it is important to assess the comparison accuracy and to insure that tolerances inherent to the method are not attributed to disagreement between the monitors. The differences between methods correspond to the ways in which point monitors are used to obtain values of the ambient trace gas concentration for use in the comparison and to the statistical treatment of this data. The sampling procedures for use with point monitors are the following:

1. Recording the real time signal from a point monitor as it is moved along the measurement path.
2. Simultaneously taking several bag samples along the path and measuring each with a point monitor.
3. Monitoring the signals from stationary point monitors placed along the measurement path.
4. Filling a sample container while moving along the measurement path and measuring the path integrated sample with a suitable point monitor.

In what follows, these various sampling procedures and the corresponding point monitor, path monitor comparison methods are discussed with special emphasis on their applicability for ozone.

In Procedure 1 a point monitor is moved with a constant velocity, V , along the measurement path, thereby describing a trajectory on the space-time graph of Figure 5, i.e., a straight line given by $S = VT$. This procedure like others using

point monitors does not give complete space-time coverage. It can be thought of as providing a number, N , of concentration measurements, A_i , along the measurement path. A specific A_i corresponds to a spatial and temporal increment and a coordinate (S_i , T_i). The average value, n_1 , obtained for the trace gas density during a transit time, T_t , is $\sum_i A_i / N$. Often the point monitor data can be obtained as an analog signal recorded on a chart recorder. In this case

$$n_1 = L^{-1} \int_{\ell=0}^L A(\ell) d\ell \quad (1)$$

where A is now a continuously recorded value for the trace gas concentration and corresponds to position along a chart trace. If conditions remain the same along the path until several traverses are made, the values of n_1 associated with a set of traverses (point monitor measurement sequence) form the statistical basis for a determination of the precision with which the true mean value of path averaged concentrations can be stated. Specifically, if a sample mean \bar{n}_1 is obtained for the individual values of n_1 , then the 95% confidence interval $\bar{n}_1 \pm \Delta_1$ includes the true mean value for 95% of all possible measurement sequences. The value of Δ_1 is given by the expression (References 1 and 2).

$$\Delta_1 = t_{.05} s_1 / k_1^{1/2} \quad (2)$$

where s_1 denotes the standard deviation for a set of traverses, k_1 denotes the number of traverses in a set, and $t_{.05}$ is a tabulated statistical function which approaches 1.96 for large k_1 .

Once the confidence interval has been defined, a formal comparison can be made between the value \bar{n}_1 and the average value, n^* , of path monitor readings during the point monitor measurement sequence. Experimentally, the number of path monitor readings is usually much greater than k_1 while the standard deviation for path monitor readings is approximately the same. Thus, the value of Δ_1 associated with the confidence interval for the path monitor is much less than in the point monitor case and the value of n^* closely approximates the true mean. For a given comparison sequence, if n^* lies within the interval $\bar{n}_1 \pm \Delta_1$ 95% of the time, then a statement that the two monitors agree can be made. Procedure 1 was used in a comparison sequence discussed in a later section of this report.

Procedure 2 involves establishing a number of stationary positions along the path at which bag samples are taken. For a bag filling time, T_f , the space-time coverage consists of vertical channels in Figure 5 corresponding to complete time coverage during T_f at the fixed sampling positions. The spatial interval Δl over which the point monitor readings are representative, i.e., the width of the vertical channels in Figure 5, is determined by the main features in the spatial gradients which exist along the path. In the case of ozone, these main features are caused by topological proximity conditions, e.g., trees or buildings which provide surfaces on which ozone is destroyed, thereby constituting an ozone "sink" and by NO source proximity such as automobile traffic near or across the measurement path. Ozone disappearance occurs when NO concentrations comparable to ambient ozone concentrations are present. In this case the rapid reaction between these two gases (Reference 3) can cause ozone changes to occur within a few seconds. Both of these causes of spatial gradients are dependent on the residence time of ozone/NO near sink/ source regions and therefore change as a result of wind speed and direction.

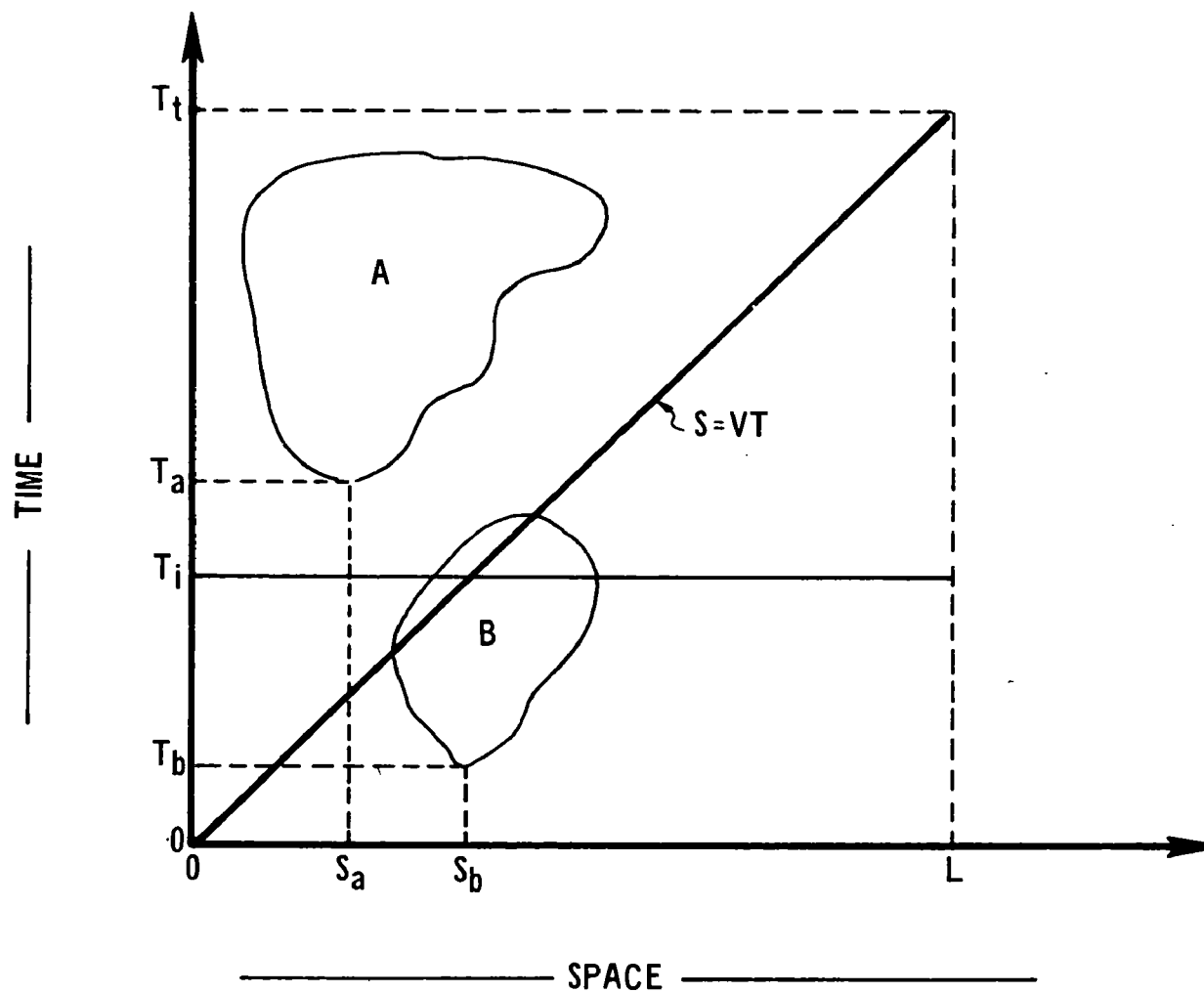


Figure 5. SPACE-TIME PLANE FOR
MEASUREMENT PATH

For Procedure 2, placement of the sampling sites must be such that spatial gradients are revealed.

Ozone concentrations must not be changed in the sampling and measurement procedure. If NO levels are high the gas phase reaction of NO and O₃ inside sample bags can reduce the O₃ level drastically. Ozone can also be destroyed on the walls of the sampling bag. Typical decay curves for 100 liter Tedlar and Mylar bags indicate that ozone decay rates can be limited to less than 8% per hour if the sample bags are conditioned with ozone prior to use and if the bags are filled to insure high volume to surface ratios.

If the sample site selection is appropriate and the integrity of bag samples is assured, an accurate point-path comparison can be made. Each bag sample measurement represents a mean ozone concentration during T_f. If T_f is short compared with temporal variations in ozone concentrations, several samples should be taken at each point. The average of a set of simultaneous samples taken along the path can be treated analogously to the path-averaged reading obtained during a traverse in Procedure 1. Each average defines a mean value n₂ so that a confidence interval n₂ ± Δ₂ can be defined based on several values of n₂. n₂ replaces n₁ and Δ₂ replaces Δ₁ in the statement on point-path comparison. If T_f is long compared with temporal ozone variations, the readings obtained from the sample bags closely approximate the true mean values at the sample sites and the sum of readings from one set of sample bags can be compared directly to an n* established during T_f.

Using Procedure 3, a close approximation to the true average trace gas concentration at some point along the measurement path can be obtained by monitoring for a time period long compared to that typical of trace gas variations. This experimental technique is illustrated for O₃ later in this section. Once these values are obtained, they are simply averaged and compared with an n* established during

the same time period. Just as in Procedure 2, stationary site locations must be adequate to accurately represent any spatial gradients. This is obviously not the case when only one or two point monitors are used along a long path near which sources and sinks of the trace gas exist. Thus, the usefulness of Procedure 3 for point-path comparisons depends on the choice of the path and prior knowledge of the temporal and spatial variability of the target gas.

Procedure 4 is useful in those cases when a portable point monitor for the target pollutant does not exist and when the path cannot be adequately characterized by sampling at a number of fixed sites. A sample container is filled as the path is traversed so that different portions of the path are equally weighted. The container is carried to a suitable point monitor and a single reading representing the target gas average along the path is obtained. Target pollutant loss while in the sample container must again be considered. However, in the case of relatively inert tracer gases or a primary pollutant such as CO, this loss can be negligible. The value of the reading obtained for each traverse, n_4 , is treated like n_1 and the comparison technique is the same as that using Procedure 1.

Measurements were made to determine the short term temporal/spatial variability of ozone. Other than diurnal variations in ozone concentration and long term trends established by NO or O₃ sources, e.g., the effect of traffic or general cloud cover patterns, variations within periods of several minutes occur which reflect localized variations in target gas concentration in the air mass being carried across measurement locations. These localized variations arise due both to disruption of the NO, NO₂, O₃, and ultraviolet radiation steady state (Reference 4) by changes in the ultraviolet throughput to ground level due to segregated clouds and to pockets of gases, e.g., NO or olefinic hydrocarbons, with which ozone reacts. These effects give rise to short term structure in the ozone concentration in both space and time.

Two ozone point monitors (Bendix Model 8002) were used in field tests to establish the variability in ambient ozone concentrations. These monitors detect ozone by its gas phase chemiluminescence with ethylene and have minimum detectable limits of less than 5.0 ppb. One monitor was placed on a stationary platform and a second one was mounted on an electric car and moved to different points along the measurement path. Figure 6 shows chart recorder traces of the two monitors as a function of time. Both monitors were stationary and they were separated by 42 meters. Variation in ozone concentrations are the result of wind conditions, of NO source and O₃ sink proximity, and of cloud cover patterns, i.e., reduction of the short wavelength radiation ($\lambda < 4000\text{\AA}$) necessary to photolyze NO₂. Air mass transport from one monitor site to the other is obvious from the time delay correlation of signal features on the two chart recordings. Correlations of this type vary depending on the projection of the wind vector along the path joining the two point monitors. Intake ports for the monitors were established at a height of six feet above the ground. These ports were open Teflon tubes of 8 mm inside diameter and approximately 100 cm long. Flow rate into the instrument was approximately 1.0 liters per minute and the time constant for the instrument was set at 1.0 seconds. With these experimental conditions the ozone concentrations monitored by the instruments were essentially real time.

In order to characterize temporal variations for one point monitor given meteorological and source/sink proximity conditions, a method of data handling was developed. A single chart recording is characterized by two quantities, an average concentration \bar{c} and a measure of the temporal variability of ozone. Data from the chart recording was digitized at six second intervals and \bar{c} was determined by averaging the set of digitized data values. The digitized readings were fitted by a linear regression analysis over a short time period, typically ten minutes. The differences

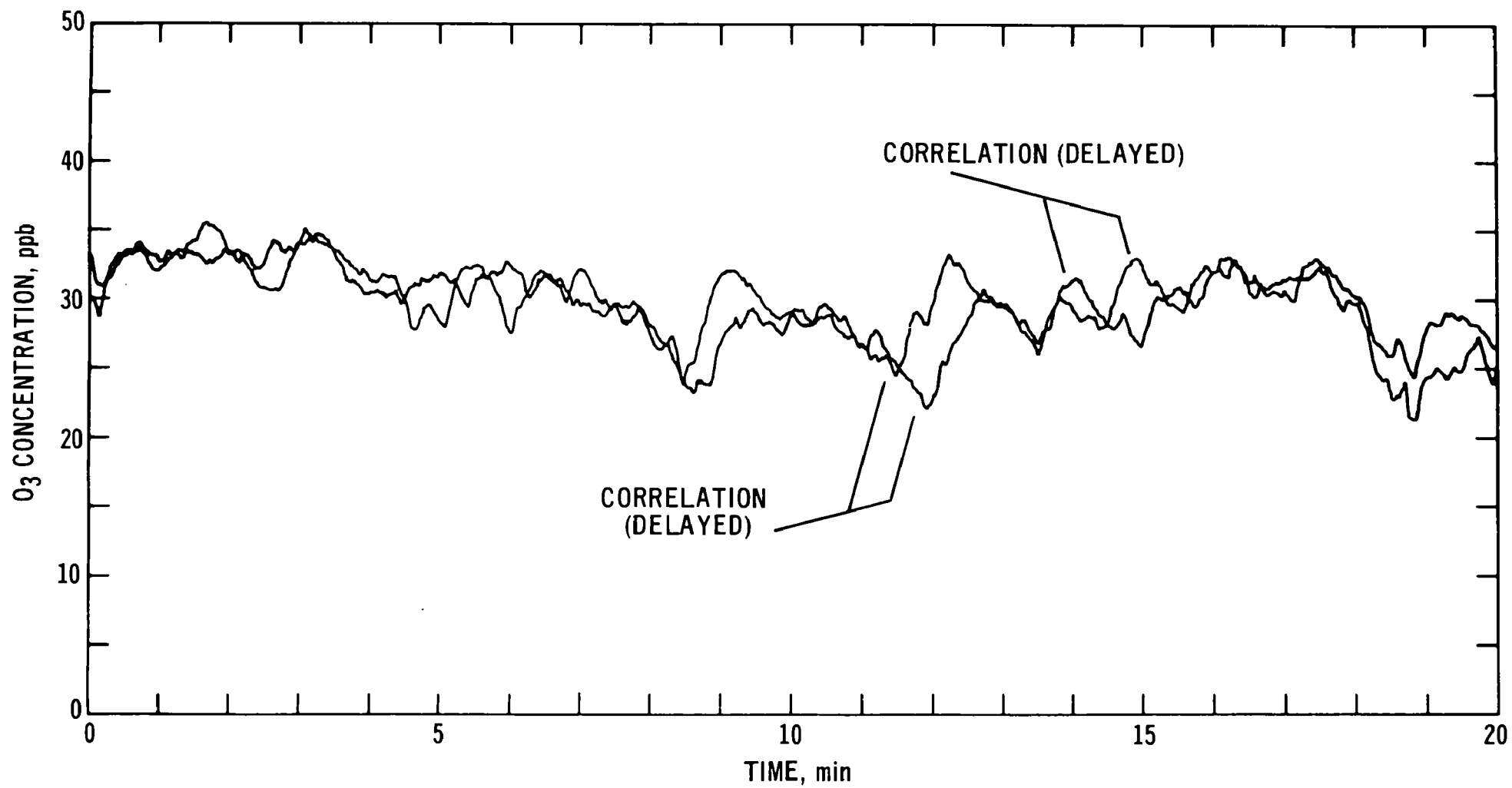


Figure 8. 100-PPM O₃ CONCENTRATION DELAYED CORRELATION ANALYSIS

between the linear approximation and actual recorded values were obtained and the number N of these differences within given intervals, Δc , of the straightline value were tabulated. The distribution of N with Δc was determined to be approximately a Gaussian distribution and hence was determined uniquely by a mean value and standard deviation. A typical distribution with a superimposed Gaussian is shown in Figure 7. As expected the standard deviation changes in response to variations in source/sink proximity conditions and in meteorological parameters such as wind speed and direction. Values of the standard deviation could be used to obtain a value of the true mean ozone concentration during the period of measurement. Typically, 100 values were determined so that a 95% confidence interval of $\bar{c} \pm 0.196s$ was defined. In most cases \bar{c} is determined within one or two ppb and can be used for point-path comparison as suggested in the discussion of Procedure 3.

Of the procedures discussed for point/path comparisons, the first and a variation of the third were used in field tests described in the next section. The major advantage in using these two procedures is that minimal ozone loss occurs due to ozone confinement prior to measurement. A secondary advantage is the requirement of only one person to perform that part of the comparison involving the point monitor. Field measurements along a measurement path of 0.67 km have indicated some of the characteristic variations in ozone concentrations to be expected. Both a hand-carried Model 560 portable ozone monitor made by Analytical Instrument Development Inc., and a Bendix Model 8002 ozone monitor were used to obtain real time ozone concentrations by moving along the measurement path. The Bendix instrument was placed on an electric car and powered by batteries with DC inverters to render it portable. A stationary monitoring station was established near one end of the measurement path as shown in Figure 8. One ozone monitor and a Climet wind speed and direction indicator were placed at the stationary site. A path along which the point monitors could be moved was established from the laser source

FIGURE 2. AMBIENT OZONE VARIATIONS
ALONG MEAN OZONE CONCENTRATIONS

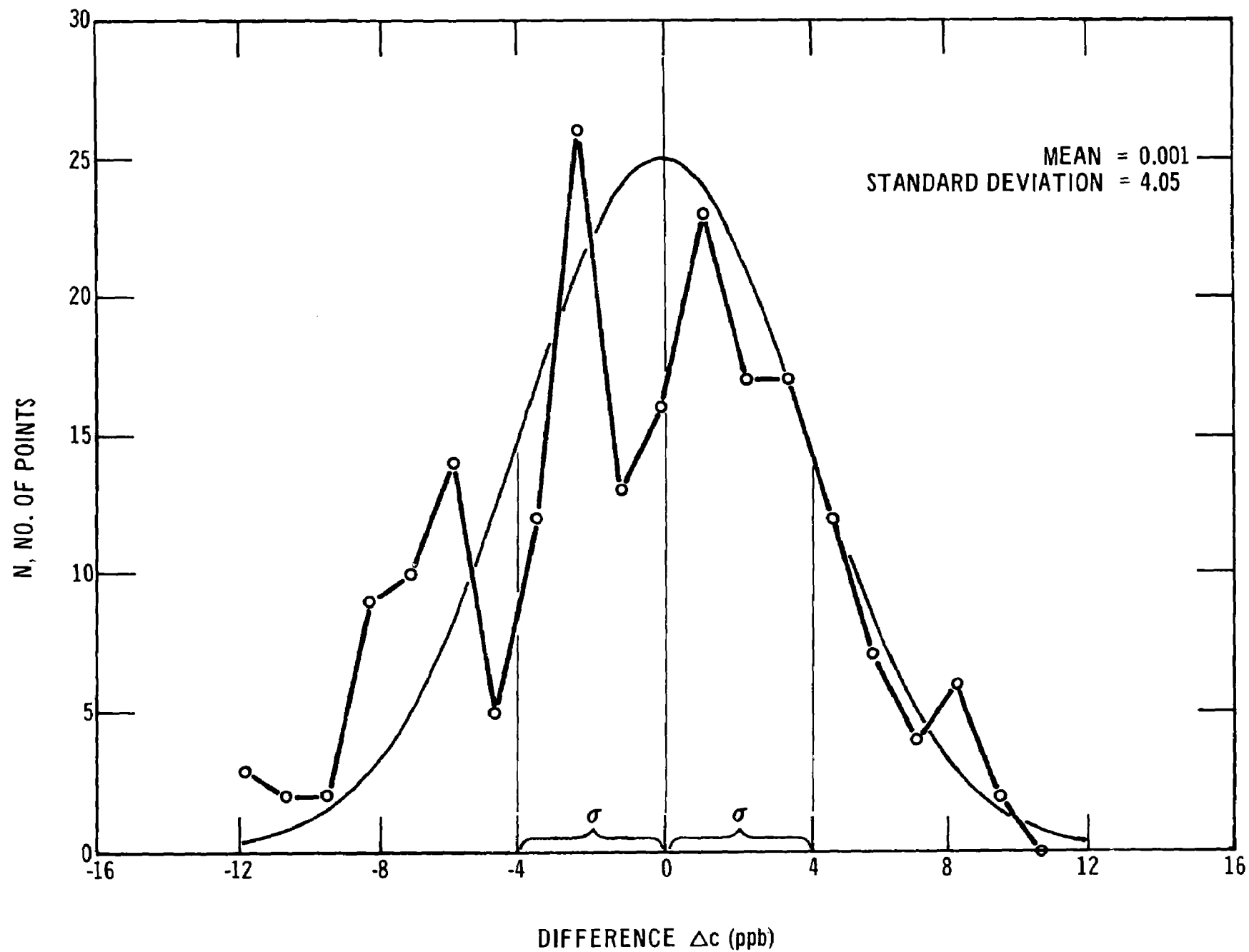
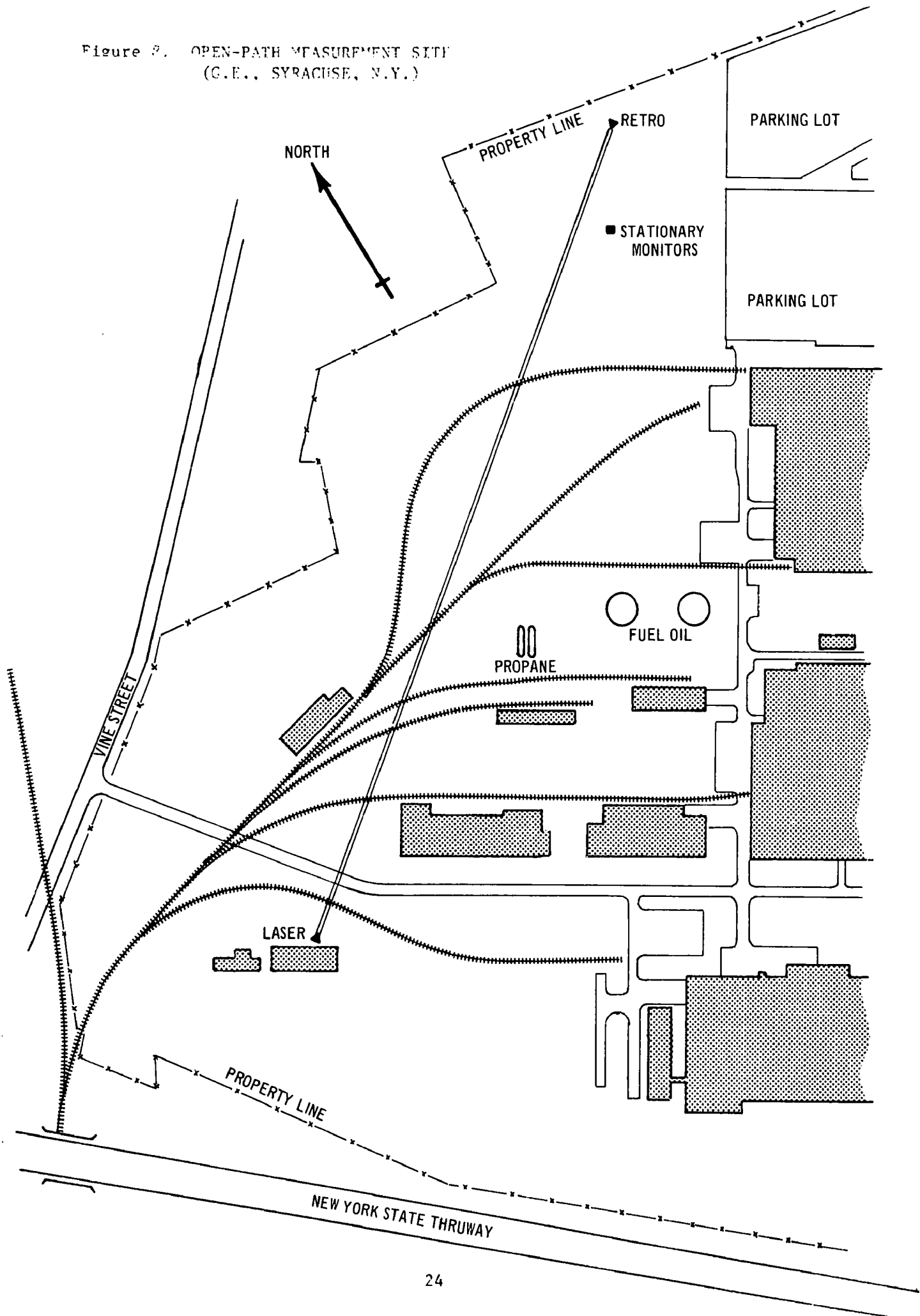


Figure 2. OPEN-PATH MEASUREMENT SITE
(G.E., SYRACUSE, N.Y.)



to its retro-reflector. Runs with the moving point monitors prior to actual comparison trials indicated that the concentration variability of ozone was strongly dependent on the wind direction and the constancy of cloud cover conditions. Arteries of traffic existed to the west and south of the stationary monitoring station while a forested residential area was to the north and east. During periods of two to three hours after 2:00 p.m. (DST) on days with consistent cloud cover, almost constant ozone concentrations existed. Consistent light wind conditions from the northeast were optimum for low ozone concentration variability.

In preparation for comparison tests, a number of simulated point monitor comparison sequences were run. The objectives of these tests were to establish the spatial gradients and the variability of ozone concentrations along the selected measurement path. The distribution of the average concentration values (n_1 values) during the individual traverses was assumed to be normal and the comparison was treated as specified in Procedure 1. Table II summarizes the point monitor data. Test 1 of Table II corresponds to the information obtained from six path traverses. A reproduction of the recorder chart outputs from these traverses are shown superimposed in Figure 9. Each trace was obtained by hand-carrying the AID ozone monitor along the measurement path of 0.67 km in a time of approximately eight minutes. A mean ozone concentration of 68.2 ppb is shown in Figure 9 along with dotted lines indicating the 95% confidence interval. For each traverse the recorder chart data was digitized to give approximately 100 values for the ozone concentration.

Test	n_1	n_1	$\Delta 1$	s_{t1}	s_{t1}	Mode	Figure
1	69.9 73.6 64.2 66.9 68.5 66.2	68.2	3.4	4.9 5.4 6.4 7.1 7.0 10.0	6.8	Moving	9
2*	62.5 63.5 64.3 65.5 64.0 63.2	63.8	1.1	1.0 2.2 2.4 1.8 2.4 2.2	2.0	Moving	10
3	68.9 70.4 70.8 69.9 70.7	70.1	1.0	2.2 2.7 2.1 2.4 2.2	2.3	Stationary	11

* Three of the traverses were made with a 1.0 second time constant and the remaining three with a 10.0 second time constant.

Table II Characterization of Ozone Variability along Measurement Path

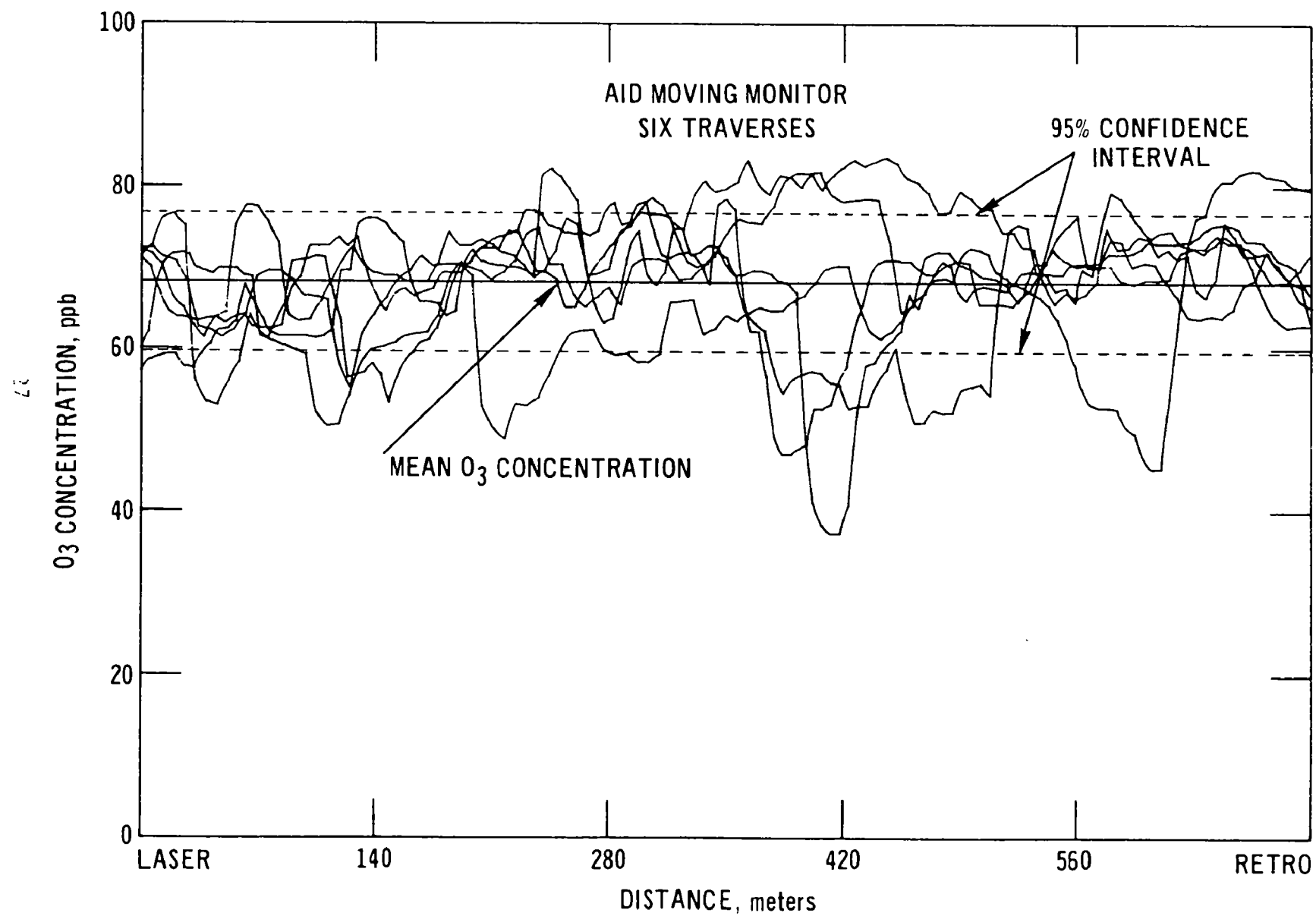


Figure 1. WEEB-TYPED RECORDED TRACES - JULY 13, 1973

The standard deviation, S_{t1} , of these values varied appreciably from traverse to traverse as seen in Table II. This variation is caused by the contribution to the concentration average of the large decreases evident in Figure 9. Decreases of this type were caused by the interaction of ozone with pockets of air having high concentrations of NO. This is an example of the practical limitation to accuracy of a comparison test in which the ambient atmospheric conditions are not sufficiently equivalent. However, in other simulated comparisons, during another day, the values of the standard deviations were approximately equal, indicating constant atmospheric conditions. Figure 10 and the corresponding treatment of the data, i.e., Test 2 of Table II illustrate this point. For Test 2, a Bendix ozone monitor with response characteristics equivalent to the AID instrument was used. The confidence interval was approximately three times smaller than that of Test 1. Thus, ambient conditions could be chosen during which the accuracy of point-path comparison sequences would be high. Specifically, the atmospheric conditions prevalent during Test 1, related mainly to wind direction, result in a wider confidence interval, $\pm \Delta$, about a sample mean than do those prevalent during Test 2.

Figure 11 shows superimposed recorder chart traces of five consecutive time intervals taken under the same atmospheric conditions as the traces of Figure 10. The data was recorded on a second Bendix ozone monitor at a stationary position along the path. Near equality of the standard deviations associated with the stationary (Test 3) and moving (Test 2) point monitors demonstrate the equivalence of temporal variability associated with a stationary monitor and the temporal-spatial variability associated with a moving point monitor.

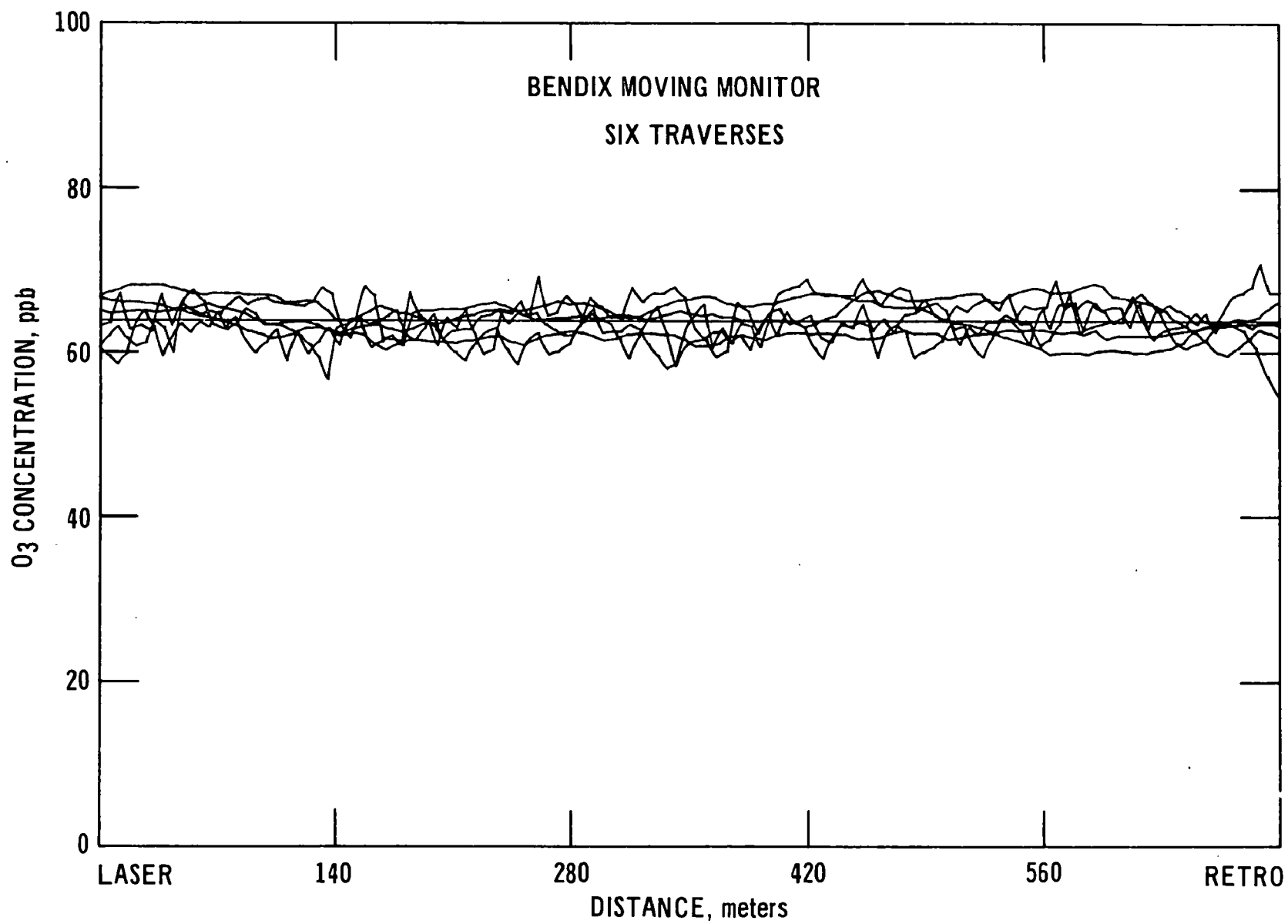


Figure 10.7 SUPER IMPOSED RECORDER - TRACES (SPACE) 11 OCTOBER 1973

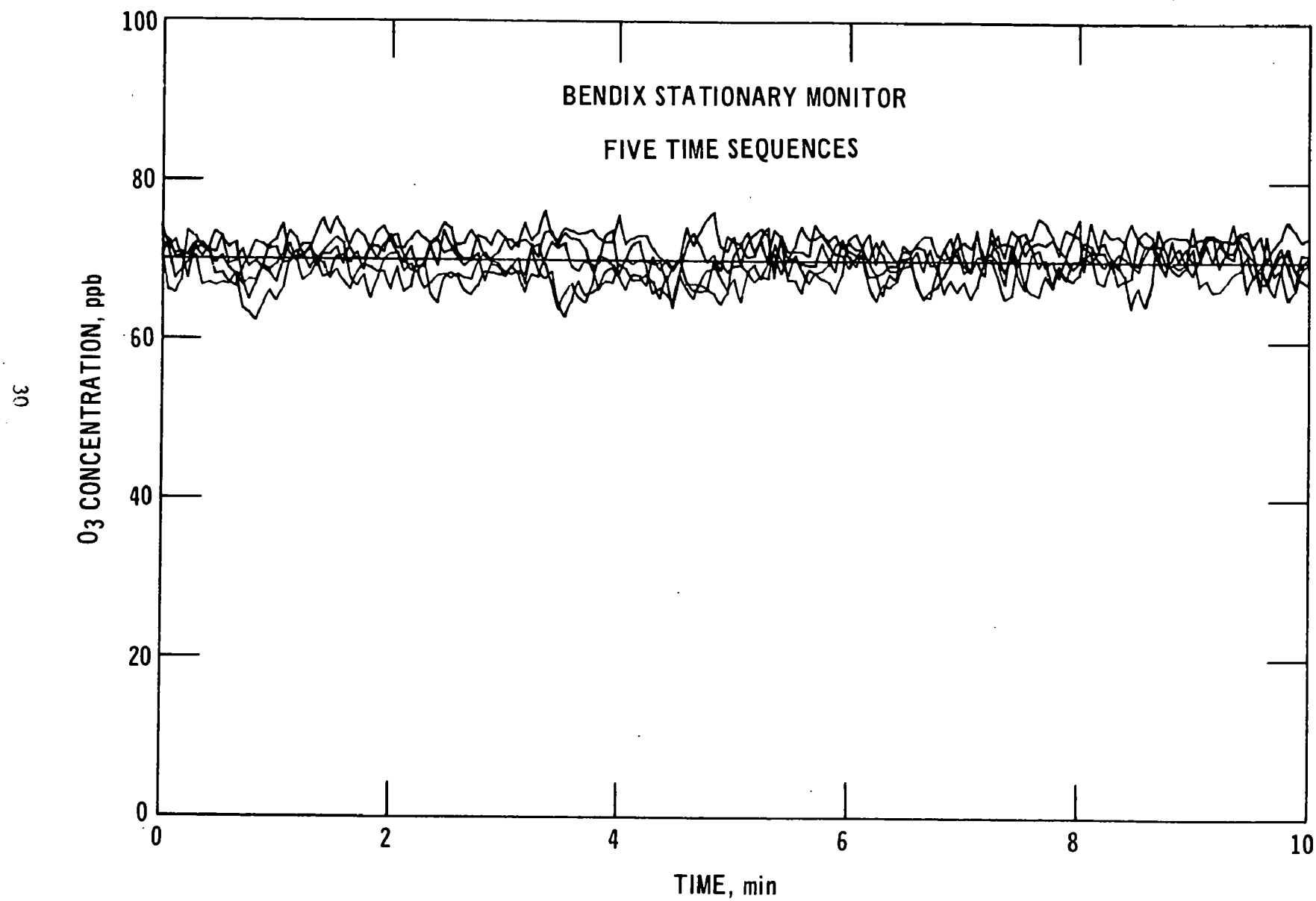


Figure 11. SUPERIMPOSED RECORDER - TRACES (TIME) - 11 OCTOBER 1973

E. FIELD MEASUREMENT RESULTS

Field tests employing ILAMS over a 0.67 km path were conducted during the period October through December of 1973. The laser beam was positioned between 1 and 2 meters above ground level and pointed along a horizontal path inside the plant boundaries of General Electric Company in Syracuse, New York. The ILAMS was housed in a small, air-conditioned trailer at one end of the path. Independent suspension of the laser and associated optics was provided in order to maintain the pointing accuracy of the laser since small changes of the order of a few thousandths of an inch at the source correspond to displacements on the order of inches at a remotely positioned retroreflector. The beam was transmitted to a two-mirror type retroreflector, consisting of an aluminized parabolic reflector of 122 cm focal length and a small secondary mirror (1.0 cm diameter) at the focal point, was positioned at the other end of the path. An area of 600 cm^2 (30 cm x 20 cm) was intercepted by the retroreflector.

Figure 12 is a picture of the system and auxiliary equipment in the trailer. Figure 13 is a view from the laser of the optical path over which ozone was measured.

Actual path/point monitor comparison tests were made in two ways. In the first, Procedure 1, described in the previous section, was used. The individual averages, n_1 were obtained by measuring the area under chart recorder traces. Two sets of six such values are shown in Tests 1 and 2 of Table III. Ozone variability was similar to that shown in Figure 9. Some variation in individual values of n_1 occurred due to changing conditions along the entire path. As specified in Procedure 1, \bar{n}_1 , and Δ_1 were determined. The average path monitor reading, n^* , during each set of six traverses was obtained by averaging a digital printout from the signal processing unit of the monitor (4 second update) which consisted of approximately 600 determinations of the path averaged ozone concentration. Under ideal test conditions n^* should fall within



Figure 12. ILAMS AND AUXILLIARY EQUIPMENT IN TRAILER - SYRACUSE, N.Y.



Figure I3. A VIEW OF THE OPTICAL PATH OVER WHICH OZONE WAS MEASURED.

Test	n_1	n_1	$\Delta 1$	n^*
1	31.6 32.6 33.8 34.1 37.7 35.1	34.2	2.2	31.3
2	49.8 56.5 43.7 43.2 44.5 47.0	47.5	5.3	49.3

Table III Point Monitor-path Monitor Comparison Data by Procedure 1

the confidence interval of n 95% of the time. For the data presented in Table III, Test 1, $n^* = 31.3$ ppb falls just outside the confidence interval 34.2 ± 2.2 ppb. For Table 2, Test 2, $n^* = 49.3$ ppb falls well within the confidence interval 47.5 ± 5.3 ppb.

To obtain a better measure of the ability of one monitor to track the other, comparison sequences during which ozone concentration gradients occur were deemed appropriate. In this case individual values of n were compared directly with n^* , i.e., the average value of the ozone concentration along the path as determined by one traverse was compared with the average value of the path monitor readings during the time of traverse. If concentration gradients do not exist, such as is the case shown in Figure 9, each point along the measurement path is equivalent. By dividing the chart recording of a single traverse into a number of segments and assigning a concentration value to each, a data base for a statistical treatment to determine the confidence interval for n is established. Equation 2 applies where now Δ defines the confidence interval about n , s denotes the standard deviation in a sample of y values for the concentration. For $y \approx 100$, $t_{.05} \approx 1.96$ and using values of s from Table II, Test 3, Δ is less than 1.0 ppb. Even with s as high as 10.0 ppb, the confidence interval is only 4 ppb.

In actual practice, the recorder chart trace for each traverse was measured with a planimeter and the value obtained was compared directly with the average of the path monitor readings during T_t . Figure 14 shows a comparison of this type extending from noon until sunset and includes the points presented in Table III as Test 2. In this comparison sequence good agreement is obtained although the disparity between path monitor and point monitor readings for several pairs of points is greater than would be expected for a common measurement path under equivalent atmospheric conditions. Review of the chart recording show that departures from equivalence occur for comparisons which show the largest disparity. In this case path monitor and point monitor may see quite different concentration profiles. This is illustrated in Figure 1 by the placement of areas labeled A. and B. Significant decreases in ozone concentration in these areas of the space-time plane will cause measurement disparities.

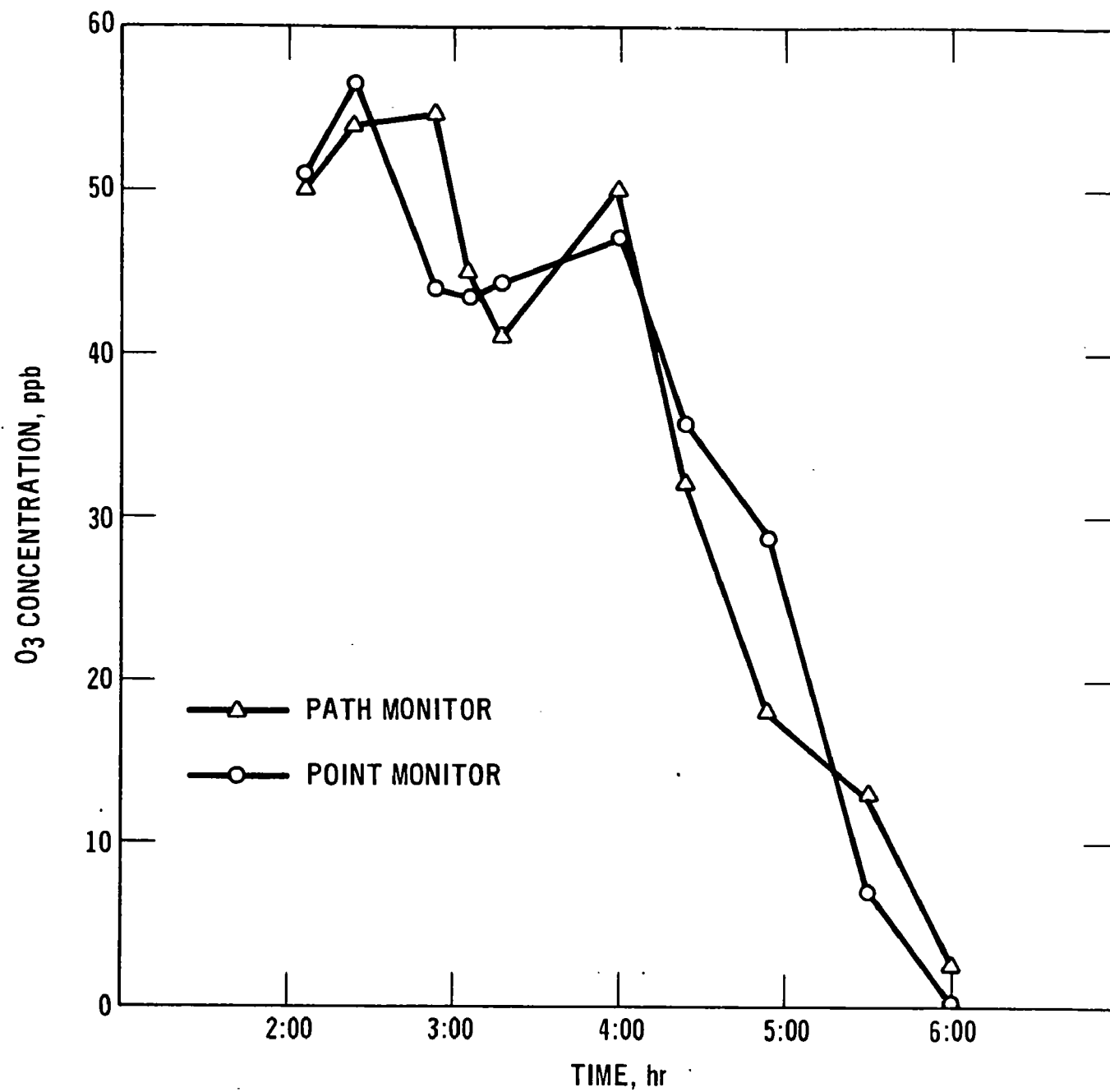


Figure 14. COMPARISON BY USE OF PROCEDURE 3

In the period following the October comparative path/point monitor tests, the ILAMS system was operated extensively. In the course of this work a number of areas were investigated. Studies of system alignment, beam position on retroreflector and distance between retro primary and secondary, were made and optimal conditions established. These studies utilized alternative entries in the Parameter Table that were preserved on paper tape for reference and future use. Laser performance was improved by adjustments and modifications. The teletype printout format was changed from 4 groups of five digits to eight groups of four digits. Other program changes to improve system performance were implemented. Minor linear weighting changes were made to correct previous errors. Signal processor sensitivity to elevated ambient temperature in the trailer was found to be caused by a defective component. System operation ended with a series of path/point monitor comparative tests 26 November through 4 December.

Again, as in the October tests, system performance effects from movement of the laser beam on the retroreflector were noted. Figure 15 shows the rapid change on the teletype printout as the beam moves off the retro. Data is from 3 December tests. Printout speed is twelve lines per minute. Each count on the left hand, ozone column, represents 2.44 ppb of O_3 . That is, 0010 indicates 24.4 parts per billion of ozone. As can be seen from the figure, in about two minutes, counts went from 0013 to 0001, a change of 29 ppb.

It is possible to compensate for beam motion through movement of the focusing lens in the system. This lens focuses the laser beam on the entrance aperture of the collimator, an off-axis parabola optical system which serves as the breadboard ILAMS transmit-receive optic. It is mounted in a fixture on the laser channel. The fixture is oriented so that the lens can be moved along the laser beam axially, vertically (V) or horizontally (H) in relation to it. Consequently, V and H axis adjustment of the focusing lens can be used to move and position the system's transmit beam on the retro.

-0013	-0005	0005	-0015	0023	-0017	0020	-0150
-0012	-0005	0004	-0017	-0011	-0043	0002	-0134
-0010	-0005	0000	-0017	0005	-0020	0002	-0166
-0012	-0005	0000	-0017	0023	-0013	0027	-0142
-0012	-0005	0004	-0017	0033	-0003	0042	-0141
-0012	-0005	0004	-0017	0036	-0023	0003	-0151
-0012	-0005	0004	-0017	0034	-0023	0046	-0140
-0012	-0005	0004	-0017	0036	-0002	0049	-0138
-0012	-0005	0004	-0017	0030	-0009	0041	-0140
-0012	-0005	0004	-0017	0027	-0011	0040	-0141
-0012	-0005	0004	-0017	0026	-0013	0039	-0142
-0013	-0005	0004	-0017	0027	-0014	0040	-0141
-0013	-0005	0004	-0017	0029	-0011	0042	-0138
-0012	-0005	0004	-0015	0024	-0017	0035	-0143
-0012	-0004	0005	-0016	0024	-0013	0030	-0145
-0012	-0004	0003	-0016	0015	-0026	0024	-0155
-0013	-0004	0003	-0015	0015	-0029	0020	-0157
-0013	-0003	0003	-0015	0030	-0014	0036	-0143
-0012	-0003	0002	-0015	0001	-0041	0005	-0173
-0011	-0003	0002	-0015	-0012	-0053	-0009	-0188
-0011	-0022	0021	-0014	-0021	-0042	0000	-0177
-0010	-0001	0001	-0014	-0013	-0051	-0014	-0193
-0009	-0001	0000	-0013	-0015	-0049	-0017	-0190
-0008	-0001	0000	-0013	-0002	-0035	-0006	-0176
-0007	0000	-0001	-0013	-0001	-0031	-0007	-0179
-0007	0000	-0001	-0013	0012	-0015	0006	-0167
-0007	-0001	0000	-0013	0040	0012	0036	-0135
-0007	-0001	0000	-0013	0057	0027	0054	-0115
-0007	-0001	0000	-0012	0038	0009	0035	-0127
-0007	-0001	0000	-0012	0023	-0000	0020	-0137
-0006	0000	-0001	-0012	0022	-0003	0016	-0144
-0005	0001	-0002	-0011	0017	-0004	0006	-0157
-0004	0002	-0003	-0010	0019	-0005	0004	-0152
-0004	0003	-0004	-0010	0018	-0005	0000	-0163
-0003	0004	-0004	-0009	0020	-0003	-0001	-0165
-0002	0004	-0005	-0009	0022	0001	-0001	-0167
-0002	0004	-0005	-0009	0021	0001	-0001	-0167
-0002	0005	-0005	-0008	0005	0004	0000	-0159
-0002	0005	-0005	-0008	0027	0004	0000	-0167
-0000	0005	-0006	-0003	0025	0005	-0002	-0171
-0001	0006	-0006	-0003	0036	0017	0000	-0154
-0001	0005	-0006	-0003	0033	0015	0005	-0153
-0001	0005	-0006	-0007	0033	0017	0005	-0153
0000	0005	-0006	-0007	0024	0000	-0003	-0193
0000	0005	-0006	-0007	0023	0000	-0003	-0189
0000	0005	-0006	-0007	0040	0031	0015	-0189
0000	0005	-0006	-0007	0064	0055	0040	-0009
0000	0004	-0005	-0007	0059	0044	0027	-0173
0000	0005	-0005	-0007	0050	0037	0020	-0170

Figure 15. SYSTEM PERFORMANCE EFFECT FROM BEAM MOVEMENT ON THE RETROREFLECTOR

Like the teletype printout, the return (analytic) signal amplitude reflects beam position on the retro. Maximum amplitude indicates the beam is centrally located on the retroreflector. With return signal amplitude oscilloscope-displayed, centering the beam on the retro can be done by V and H axis adjustment of the focussing lens. This approach was used to check beam position and center the beam on the retro. Signal amplitude variation with V and H movement was an indication of beam location relative to the retro center. Thus, maximizing or "peaking" the signal on the oscilloscope with V and H adjust would center the beam. When centering the beam, it was decided that final V and H settings would be the mid-point between the micrometer screw settings where the return signal rose and fell significantly as the beam was moved across the retro by the motion of axes adjustment screws.

A series of comparative path-point monitor field tests in the period 26 November through 4 December duplicated some of the results obtained in October and provided additional information on the system's performance. Comparative data was collected in the same manner as that employed in the earlier tests. Retroreflector alignment checks, secondary mirror position relative to primary, took place 28 November. The secondary was moved .025 inches further away from the primary. Also a weight change was made on the ozone channel to reflect an earlier shift in λ , from the R14 line to the R16 line of the $(00^0_1 - 02^0_0)$ transition. In microns, the wavelength shift was from 9.3054 to 9.2938. It was made to avoid water vapor interference noted after the original wavelength selection process was completed.

The weather during this period in November and early December was quite variable with snow and rain occurring. The system was operative in all but extreme weather conditions, even when the retroreflector site was not visible from the trailer. December 3rd was an unusually warm winter day. The high temperature was 58° F, a near-record for Syracuse. It was bright and sunny, reminiscent of important data-taking days in late October. The laser was turned on at 0650. The system was balanced at 0830. Around 0900 a steady negative drift in concentration-related counts on the teletype printout prompted frequent checks of beam position on the retroreflector throughout the day.

The comparative data for this day is shown in Figure 16. Noteworthy is the general absence of large excursions in path monitor relative to point monitor data noted in October data during mornings and late afternoons. (It was felt that adjustment of beam position in the period 1345 to 1430 could have been more frequent to reduce the excursion at 1428 on the figure). Table IV shows beam position shift with time of day in terms of focussing lens adjustments made to maximize the return signal. Note that H axis adjustment is constant (within operator reading error tolerance for an awkward location) while V axis setting rises and falls with time of day and coincidentally, the effect of localized atmospheric heating. This represents about a seven centimeter beam excursion on the retro. Similar data for 23 October shows the laser beam raised 15 centimeters on the retroreflector. As the retro diameter was 20 centimeters, this motion could be expected to have considerable effect on the system. The time of day variation in beam position gives rise to speculation that beam motion at the retro is largely attributable to atmospheric looming.

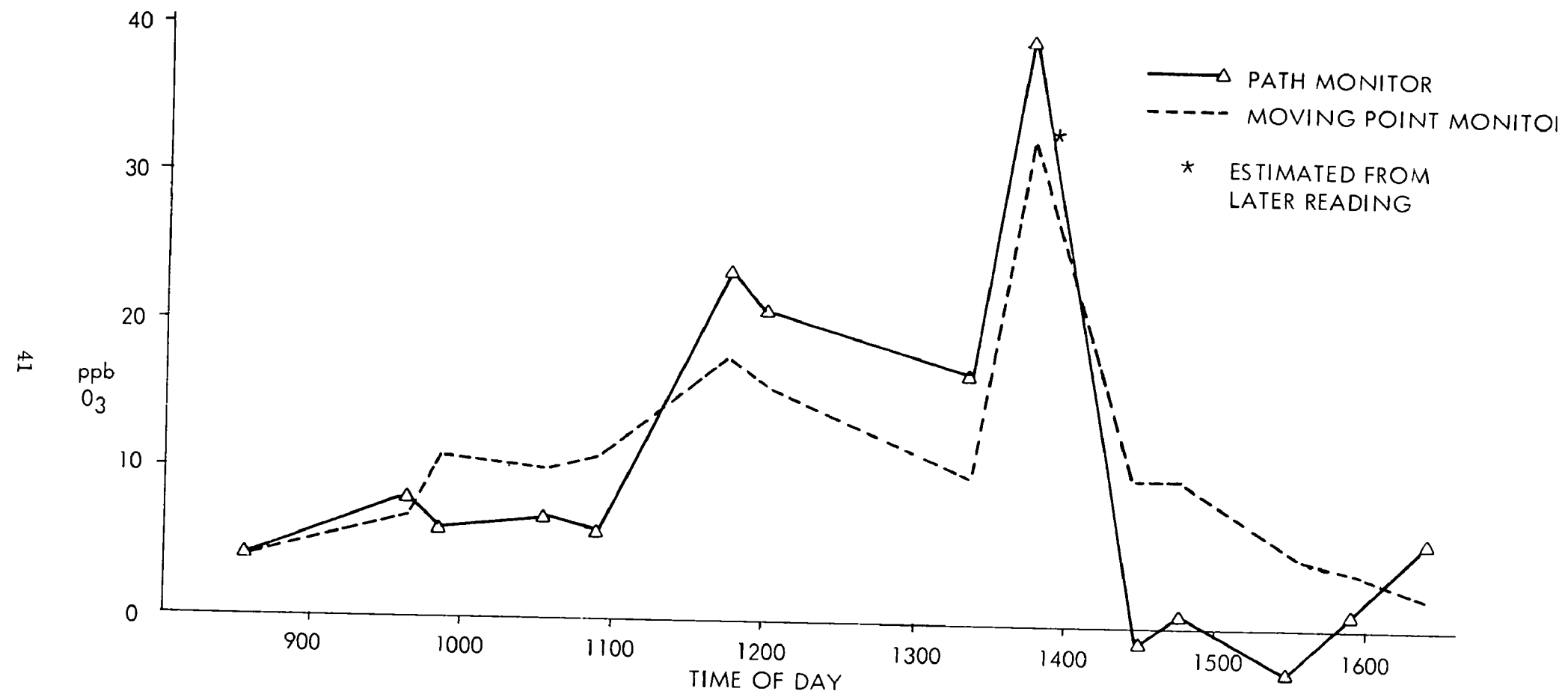


Figure 16. COMPARATIVE PATH/MOVING POINT MONITOR OZONE DATA - 3 DEC 1973

3 December 1973

Time	V	H
Start*	379.6	308.5
0815	376.5	308.4
0928	378.0	308.5
1006	378.9	308.4
1022	no change	
1135	379.6	308.4
1259	no change	
1410	379.3	308.5
1440	379.0	308.5
1513	378.5	308.5
1540	378.0	308.5
1615	377.4	308.5

* Laser was turned on at 0650. Initial V and H settings were those made at 1520 30 November.

Table IV Shift of Beam Position on Retroreflector with Time of Day as Indicated by Focusing Lens Adjustment

F. CONCLUSIONS

An example of point monitor and path monitor comparisons is shown in Figure 17. It includes the afternoon data of Figure 14 with the morning data taken on 23 October. The erratic behavior of the ILAMS during the morning hours has not been definitely identified, but is believed to be related to the alignment of the laser beam at the retroreflector. Spurious absorptions result whenever the relationship between return and reference signals are changed by other than known atmospheric attenuators. In this case the spurious absorption coincided with drift of the transmitted laser beam away from the retroreflector caused by atmospheric looming as the ground warmed up and cooled down during the day to produce vertical temperature gradients in the system's optical path.

The accuracy with which measurement of ozone concentrations could be made was limited by optical noise related to atmospheric turbulence and thermal gradients. The transmit and receive optics produced spectral attenuation because the diameter of the far field diffraction pattern of the laser beam is proportional to wavelength. The retroreflector is an aperture stop that acts upon these spatial variations to produce spectral attenuation. Hence, when the transmitted beam was focused on the retroreflector, one would expect a spectral return in the presence of atmospheric looming, which is precisely what we observed. It was shown possible to produce a similar error by deliberately aiming the beam slightly off the edge of the retroreflector. The experiments with defocusing the beam to alleviate this problem, however, resulted in an increase in the observed optical noise and an increase in measurement error. The aggravation of the noise condition with defocusing indicated that spectral non-uniformities were still present in the near field in spite of the spatial filter (clean up aperture) in the laser transmitter. Direct

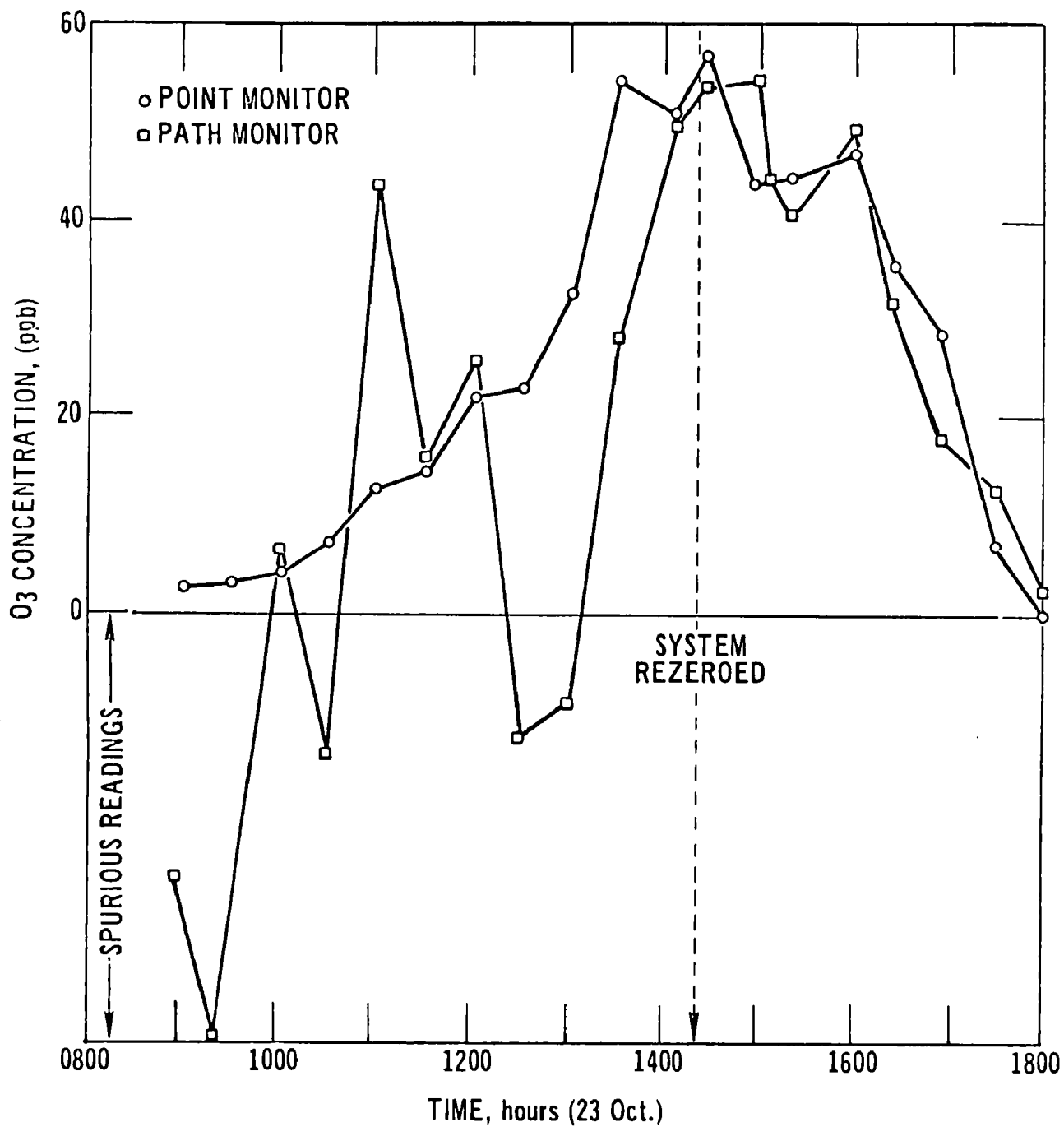


Figure 17. POINT AND PATH MONITOR COMPARISON

measurements of the intensity pattern of the near field showed that there is indeed some "clutter" in the near field beam and this has been tentatively attributed to the optical surfaces of the laser transmitter both preceding and following the clean up aperture.

The signal output of this laser detection system is proportional to the log of the ratio of the signal returned from the retroreflector to the signal on the reference detector. Since it is the relative signal behavior of the two detectors to which the output is sensitive, it is equally possible that drift in the optics preceding the reference detector is also partially responsible for the measured error in the output. However, because the major drift error occurred in the mornings on clear days following clear nights, the strong change in humidity and ground temperature during the morning hours are considered significant.

Water vapor is fairly well understood spectral interference, but ground fog and liquid water adhering to particulates (haze) is not. In addition, unknown spectral interferences may have entered the beam to offset the system's zero baseline. (A method called factor analysis, to analyze and compensate for unknown spectral effects is discussed in Volume I).

The effect of looming on the laser beam was noted on many occasions. Direct measurement of the effect has been reported in the previous section. Reaiming the laser by moving the focussing lens preceding the beam expander to correct for the looming only appeared to compensate for about 50% of the measurement error associated with this time of day phenomenon. The considerable drift in the laser system output signal which has been tentatively attributed to looming was greatest during the mornings on clear days when the wind velocity was low. In these periods, the RMS error between the ILAMS and the point monitor ozone measurements was approximately 28 parts per billion. At other times, the system was relatively stable and the RMS error was about 6 parts per billion. It is expected that the effects of atmospheric looming on the signal are still the dominant source of error even during stable operation and that correcting non-uniformities in the transmitted laser beam will reduce the system error and improve its accuracy.

REFERENCES

1. G.W. Snedecor, Statistical Methods, The Iowa State College Press, Ames, Iowa.
2. B.E. Saltzman, Journal of the Air Pollution Control Association, 22 (No. 2), 90, February 1972.
3. J.A. Ghormley, R.L. Ellsworth, and C.J. Hochanadel, J. Phys. Chem., 77, 1341, 1973.
4. D.H. Stedman, E.E. Daby, F. Stuhl, and H. Niki, Journal of the Air Pollution Control Association, 22 (No. 4), 260, April 1972.
5. Final Report: Field Study on Application of Laser Coincidence Absorption Measurement Techniques, Contract EHSD 71-8, February 1972, prepared for the Environmental Protection Agency by General Electric Electronics Laboratory, Syracuse, N.Y. The system used in the comparison tests is a modified form of the system described in this final report. Modifications include those specified in Reference 5.

TECHNICAL REPORT DATA (Please read Instructions on the reverse before completing)		
1. REPORT NO. EPA-650/2-74-046-b	2.	3. RECIPIENT'S ACCESSION NO.
4. TITLE AND SUBTITLE Development of a Gas Laser System to Measure Trace Gases by Long Path Absorption Techniques Volume II Field Evaluation of Gas Laser System for Ozone Monitoring		5. REPORT DATE July 1974
		6. PERFORMING ORGANIZATION CODE
7. AUTHOR(S) W. A. McClenny, F. W. Baity, Jr., R. E. Baumgardner, Jr., R. A. Gray, EPA, R. J. Gillmeister and L. R. Snowman, G. E.		8. PERFORMING ORGANIZATION REPORT NO.
9. PERFORMING ORGANIZATION NAME AND ADDRESS Joint Report: Environmental Protection Agency, Research Triangle Park, North Carolina 27711 and General Electric Company, Electronic Systems Division, Pittsfield, Massachusetts 01201		10. PROGRAM ELEMENT NO. 1AA010
		11. CONTRACT/GRANT NO. 68-02-0757
12. SPONSORING AGENCY NAME AND ADDRESS Environmental Protection Agency National Environmental Research Center Chemistry and Physics Laboratory Research Triangle Park, North Carolina 27711		13. TYPE OF REPORT AND PERIOD COVERED Final
		14. SPONSORING AGENCY CODE
15. SUPPLEMENTARY NOTES Joint Field Study by G. E. and EPA of Open-Path Monitor		
16. ABSTRACT Ambient ozone measurements in real time using an open-path monitor are described. These studies establish the sensitivity of an open-path monitor, based on transmissivity measurements of CO ₂ laser lines, at ≤ 5 ppb and validate the values obtained during real-time monitoring of ambient ozone by establishing and using a methodology for the comparison of point monitor readings and open-path monitor readings over a common path.		
17. KEY WORDS AND DOCUMENT ANALYSIS		
a. DESCRIPTORS Lasers Atmospheric Absorption Ozone Air Pollution Monitoring	b. IDENTIFIERS/OPEN ENDED TERMS ILAMS Methodology for Point Monitor, Path Monitor Comparisons	c. COSATI Field/Group 1705
18. DISTRIBUTION STATEMENT Release Unlimited	19. SECURITY CLASS (This Report) Unclassified	21. NO. OF PAGES 51
	20. SECURITY CLASS (This page) Unclassified	22. PRICE

INSTRUCTIONS

1. **REPORT NUMBER**
Insert the EPA report number as it appears on the cover of the publication.
2. **LEAVE BLANK**
3. **RECIPIENTS ACCESSION NUMBER**
Reserved for use by each report recipient.
4. **TITLE AND SUBTITLE**
Title should indicate clearly and briefly the subject coverage of the report, and be displayed prominently. Set subtitle, if used, in smaller type or otherwise subordinate it to main title. When a report is prepared in more than one volume, repeat the primary title, add volume number and include subtitle for the specific title.
5. **REPORT DATE**
Each report shall carry a date indicating at least month and year. Indicate the basis on which it was selected (*e.g., date of issue, date of approval, date of preparation, etc.*).
6. **PERFORMING ORGANIZATION CODE**
Leave blank.
7. **AUTHOR(S)**
Give name(s) in conventional order (*John R. Doe, J. Robert Doe, etc.*). List author's affiliation if it differs from the performing organization.
8. **PERFORMING ORGANIZATION REPORT NUMBER**
Insert if performing organization wishes to assign this number.
9. **PERFORMING ORGANIZATION NAME AND ADDRESS**
Give name, street, city, state, and ZIP code. List no more than two levels of an organizational hierarchy.
10. **PROGRAM ELEMENT NUMBER**
Use the program element number under which the report was prepared. Subordinate numbers may be included in parentheses.
11. **CONTRACT/GRANT NUMBER**
Insert contract or grant number under which report was prepared.
12. **SPONSORING AGENCY NAME AND ADDRESS**
Include ZIP code.
13. **TYPE OF REPORT AND PERIOD COVERED**
Indicate interim final, etc., and if applicable, dates covered.
14. **SPONSORING AGENCY CODE**
Leave blank.
15. **SUPPLEMENTARY NOTES**
Enter information not included elsewhere but useful, such as: Prepared in cooperation with, Translation of, Presented at conference of, To be published in, Supersedes, Supplements, etc.
16. **ABSTRACT**
Include a brief (*200 words or less*) factual summary of the most significant information contained in the report. If the report contains a significant bibliography or literature survey, mention it here.
17. **KEY WORDS AND DOCUMENT ANALYSIS**
 - (a) **DESCRIPTORS** - Select from the Thesaurus of Engineering and Scientific Terms the proper authorized terms that identify the major concept of the research and are sufficiently specific and precise to be used as index entries for cataloging.
 - (b) **IDENTIFIERS AND OPEN-ENDED TERMS** - Use identifiers for project names, code names, equipment designators, etc. Use open-ended terms written in descriptor form for those subjects for which no descriptor exists.
 - (c) **COSATI FIELD GROUP** - Field and group assignments are to be taken from the 1965 COSATI Subject Category List. Since the majority of documents are multidisciplinary in nature, the Primary Field/Group assignment(s) will be specific discipline, area of human endeavor, or type of physical object. The application(s) will be cross-referenced with secondary Field/Group assignments that will follow the primary posting(s).
18. **DISTRIBUTION STATEMENT**
Denote releasability to the public or limitation for reasons other than security for example "Release Unlimited." Cite any availability to the public, with address and price.
19. & 20. **SECURITY CLASSIFICATION**
DO NOT submit classified reports to the National Technical Information service.
21. **NUMBER OF PAGES**
Insert the total number of pages, including this one and unnumbered pages, but exclude distribution list, if any.
22. **PRICE**
Insert the price set by the National Technical Information Service or the Government Printing Office, if known.